

See discussions, stats, and author profiles for this publication at: <https://www.researchgate.net/publication/274006400>

Exploring Self-Condensing Vinyl Polymerization of Inimers in Microemulsion To Regulate the Structures of Hyperbranched Polymers

ARTICLE in *MACROMOLECULES* · MARCH 2015

Impact Factor: 5.8 · DOI: 10.1021/acs.macromol.5b00278

CITATIONS

4

READS

42

3 AUTHORS, INCLUDING:



[Robert William Graff](#)

University of Notre Dame

12 PUBLICATIONS 16 CITATIONS

SEE PROFILE



[Xiaofeng Wang](#)

University of Notre Dame

10 PUBLICATIONS 20 CITATIONS

SEE PROFILE

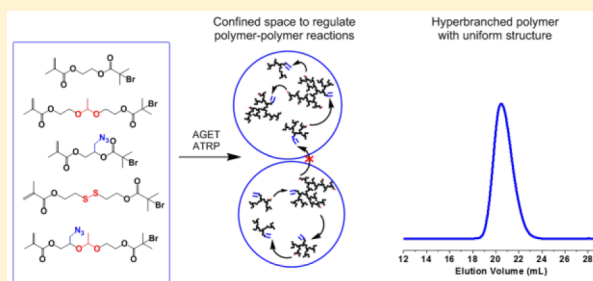
Exploring Self-Condensing Vinyl Polymerization of Inimers in Microemulsion To Regulate the Structures of Hyperbranched Polymers

Robert W. Graff, Xiaofeng Wang, and Haifeng Gao*

Department of Chemistry and Biochemistry, University of Notre Dame, Notre Dame, Indiana 46556, United States

S Supporting Information

ABSTRACT: A synthetic method was successfully developed to produce structurally defined hyperbranched polymers using confined micellar space in microemulsion to regulate atom transfer radical polymerization (ATRP) of inimers. Systematic exploration of experimental variables, including five methacrylate-based inimer species, two ATRP ligands, and varied amounts of inimers and catalysts, produced a series of hyperbranched polymers that encompassed a broad range of molecular weights ($M_n = 194$ –1301 kg/mol), high degrees of branching ($DB = 0.26$ – 0.41), and narrow molecular weight distribution ($M_w/M_n = 1.1$ – 1.7). The ATRP of inimers in the microemulsion media showed a fast polymerization rate with quantitative conversion of methacrylate groups within 0.5 h. At high conversion, there was essentially one hyperbranched polymer per discrete latex particle, whose dimension (hydrodynamic diameter $D_h = 10.95$ – 20.13 nm in water) and uniformity directly determined the molecular weight and polydispersity of the hyperbranched polymer. The DB of hyperbranched polymers was quantitatively determined using inverse gated ^{13}C NMR spectroscopy, and its value was affected by several parameters, all related to the effective amount of copper catalysts in the polymerization loci for dynamic ATRP exchange reactions. The use of inimers and ligands that showed high copper complex solubility and a high feed ratio of copper to inimer could increase the concentration of copper catalyst in the discrete particles and consequently the DB value. Within the investigation, the polymerization of inimer 3 using 4,4'-dinonyl-2,2'-dipyridyl (dNbpy) as ligand produced hyperbranched polymers with the highest $DB = 0.41$ due to the high solubility of $\text{Cu(II)}/(\text{dNbpy})_2$ in inimer 3. When acetal group as a linker was incorporated into the inimer, the produced hyperbranched polymers exhibited complete degradation in acidic environment, indicating potential utility in biomedical applications.



INTRODUCTION

Both dendrimers and hyperbranched polymers are considered as important types of highly branched polymers that show compact structures, large interior volumes, and multiple chain-end groups.^{1–5} However, these two types of polymers differ on many aspects. Dendrimers feature a perfectly branched and monodisperse structure by means of multistep iterative synthesis.^{2,6,7} In contrast, hyperbranched polymers have a straightforward one-pot synthesis but limited control over their molecular weight, molecular weight distribution, and branching density.^{3,4,8} It has been a challenging problem for years to develop robust synthetic methods that can produce hyperbranched polymers in one-pot with better controlled structures.⁹

Hyperbranched polymers are traditionally synthesized in solution using the step-growth polymerization of AB_f monomers (containing one A group and f (≥ 2) B groups)^{3,4,10,11} and/or self-condensing vinyl polymerization (SCVP) of AB^* inimers (containing initiator fragment B^* and monomer vinyl group A in one molecule).^{12–14} In both cases, the polymers present undesirable structures with broad molecular weight distributions,¹⁵ mainly due to the random polymer–polymer coupling reactions occurring in the continuous reaction media throughout

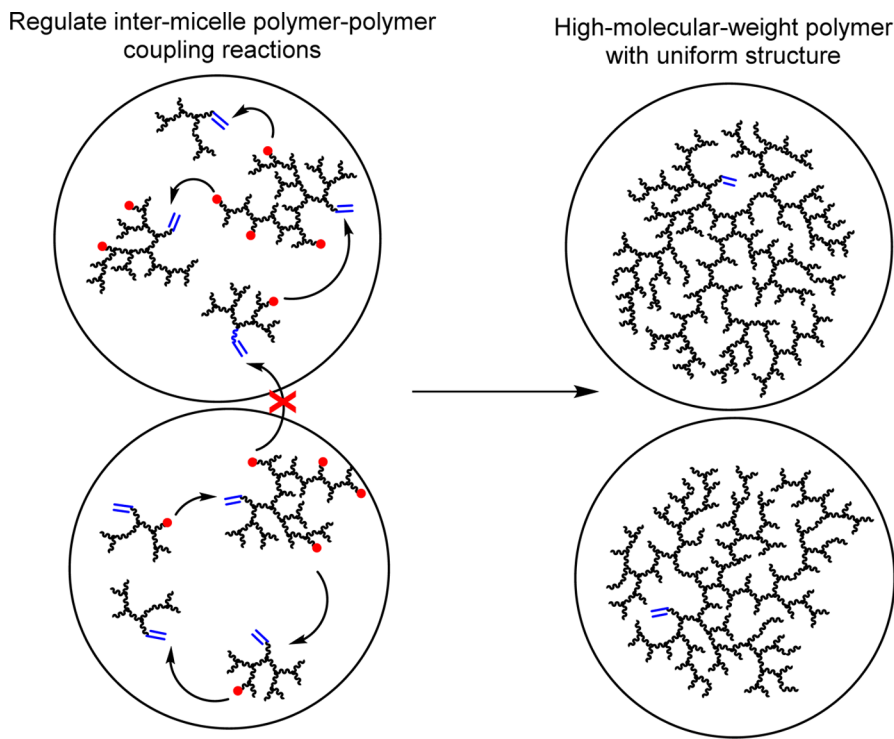
the polymerization.¹² In the past two decades, considerable efforts have been reported to decrease the polydispersity^{16,17} and increase the degree of branching (DB) of the hyperbranched polymers using multifunctional cores,^{18,19} tuning the monomer addition speed,^{18,20} and varying the monomers' reactivity.^{21,22} However, all these methods require either delicate monomer addition or sophisticated monomer synthesis,⁹ which limit the synthetic ease and the production of hyperbranched polymers with high molecular weights.

Recently, our group developed a new approach to synthesize hyperbranched polymers with both high molecular weight and narrow molecular weight distribution using confined nanospace, e.g., micelles, to regulate the polymer–polymer coupling reactions.²³ The key concept in this new method is to segregate the polymerization of reactive monomers into discrete micelles, so that the monomers inside each micelle or polymerizing locus can react/polymerize with each other completely, while there is no intermicelle reaction. In this present report, we systematically

Received: February 9, 2015

Revised: March 11, 2015

Scheme 1. Illustration of Polymerization of Inimers in Confined Space



investigated this novel synthetic method by exploring various experimental conditions. The new method exhibited great versatility in the polymerization of different inimers and produced a series of hyperbranched polymers with varied compositions, structures ($DB = 0.26\text{--}0.41$), molecular weights ($M_n = 194\text{--}1301$ kg/mol), and low polydispersity ($M_w/M_n = 1.1\text{--}1.7$), which have not been reported in the literature using other one-pot synthetic methods.

EXPERIMENTAL SECTION

Materials. All chemicals and solvents, including 4,4'-dinyon-2,2'-dipyridyl (dNbpy), CuBr_2 , sodium ascorbate (NaAs), and polyoxyethylene(20) oleyl ether (Brij98), were purchased from Aldrich with the highest purity and used as received unless otherwise stated. Bis(2-pyridylmethyl)octadecylamine (BPMODA) was synthesized according to similar procedures previously published.²⁴

Characterization. Monomer conversions were determined from the concentration of unreacted monomers in the samples, which were periodically removed from the reactions, using a Bruker 500 MHz NMR spectrometer. After filtration through $0.45\ \mu\text{m}$ PTFE filter, the polymer samples were separated by size exclusion chromatography (SEC) with THF as mobile phase. The THF SEC was equipped with Polymer Standards Services (PSS) columns (guard, 10^5 , 10^3 , and 10^2 Å SDV columns) at $35\ ^\circ\text{C}$ with THF flow rate = $1.00\ \text{mL/min}$ and a differential refractive index (RI) detector (Wyatt Technology, Optilab T-rEX) using PSS WinGPC 7.5 software. The apparent molecular weights were calculated based on linear poly(methyl methacrylate) (PMMA) standards. The detectors employed to measure the absolute molecular weights of hyperbranched polymers in THF SEC were the RI detector and a multiangle laser light scattering (MALLS) detector (Wyatt Technology, DAWN HELEOS II) with the light wavelength at $658\ \text{nm}$. Absolute molecular weights were determined using ASTRA software from Wyatt Technology with the $dn/dc = 0.084\ \text{mL/g}$ for all polymethacrylate-based polymers.^{25,26} ^1H NMR, ^{13}C NMR, heteronuclear multiple-bond correlation (HMBC), heteronuclear single-quantum coherence (HSQC), and inverse gated decoupled ^{13}C NMR spectra (relaxation period $d_1 = 20\ \text{s}$) were acquired with CDCl_3 as solvent on a Bruker 500 MHz spectrometer at $25\ ^\circ\text{C}$. The hydrodynamic

size and coefficient of variation (CV) of the samples were determined using dynamic light scattering (DLS) equipped with a Zetasizer Nano-ZS (He-Ne laser wavelength at $633\ \text{nm}$, Malvern Instruments, Malvern, UK).

Synthesis of 2-(2-Bromoisobutyryloxy)ethyl Methacrylate (Inimer 1).²⁷ A 100 mL round-bottom flask was loaded with a magnetic stir bar, 2-hydroxyethyl methacrylate ($12.13\ \text{mL}$, $0.10\ \text{mol}$), pyridine ($8.60\ \text{mL}$, $0.11\ \text{mol}$), and $70\ \text{mL}$ of dichloromethane (DCM), before being cooled to $0\ ^\circ\text{C}$ in an ice bath. 2-Bromoisobutyryl bromide ($12.36\ \text{mL}$, $0.10\ \text{mol}$) was dissolved in $15\ \text{mL}$ of DCM and added to the reaction mixture via an addition funnel over $45\ \text{min}$. The reaction was kept cold for an additional $45\ \text{min}$ before being warmed up to room temperature for an additional $3\ \text{h}$. After the reaction, the solvent was removed under reduced pressure before the product was purified on a silica column (4:1 hexanes:ethyl acetate), obtaining $25.68\ \text{g}$ of clear oil (92% yield). 500 MHz ^1H NMR spectroscopy (δ , CDCl_3 as solvent): $6.07\ \text{ppm}$ (m, 1H, $\text{CH}_2=\text{C}(\text{CH}_3)$), $5.52\ \text{ppm}$ (m, 1H, $\text{CH}_2=\text{C}(\text{CH}_3)$), $4.35\ \text{ppm}$ (m, 4H, $\text{OCH}_2\text{CH}_2\text{O}$), $1.88\ \text{ppm}$ (s, 3H, $\text{CH}_2=\text{C}(\text{CH}_3)$), and $1.86\ \text{ppm}$ (s, 6H, $\text{C}(\text{CH}_3)_2\text{Br}$).

Synthesis of 2-(Vinylloxy)ethyl 2-Bromo-2-methylpropanoate. A 100 mL round-bottom flask was loaded with magnetic stir bar, 2-(vinylloxy)ethanol ($5.00\ \text{mL}$, $0.056\ \text{mol}$), TEA ($7.76\ \text{mL}$, $0.056\ \text{mol}$), and $20\ \text{mL}$ of DCM before being cooled to $0\ ^\circ\text{C}$ in an ice bath. A mixture of 2-bromoisobutyryl bromide ($6.88\ \text{mL}$, $0.056\ \text{mol}$) was dissolved in $5\ \text{mL}$ of DCM and added to the reaction mixture via an addition funnel over $30\ \text{min}$. The reaction was then warmed up to room temperature and reacted overnight before filtration of the solid and removal of solvent under reduced pressure. The product was purified via distillation under reduced pressure at $70\ ^\circ\text{C}$ yielding $9.99\ \text{g}$ of clear oil (73% yield). 500 MHz ^1H NMR spectroscopy (δ , CDCl_3 as solvent): $6.46\ \text{ppm}$ (dd, 1H, $\text{OCH}=\text{CH}_2$), $4.39\ \text{ppm}$ (t, 2H, COOCH_2), $4.20\ \text{ppm}$ (dd, 1H, $\text{CH}_2=\text{CHO}$), $4.35\ \text{ppm}$ (dd, 1H, $\text{CH}_2=\text{CHO}$), $3.92\ \text{ppm}$ (t, 2H, OCH_2CH_2) and $1.93\ \text{ppm}$ (s, 6H, $\text{C}(\text{CH}_3)_2\text{Br}$).

Synthesis of 2-(1-(2-(2-Bromo-2-methylpropanoyloxy)ethoxy)ethoxy)ethyl Methacrylate (Inimer 2).²⁸ 2-(Vinylloxy)ethyl 2-bromo-2-methylpropanoate ($3.80\ \text{g}$, $0.016\ \text{mol}$) and 2-hydroxyethyl methacrylate ($2.085\ \text{g}$, $0.016\ \text{mol}$) were dissolved in $50\ \text{mL}$ of DCM. A catalytic amount of *p*-toluenesulfonic acid ($30.5\ \text{mg}$, $0.16\ \text{mmol}$) was added to start the reaction. The reaction was allowed to stir for $1\ \text{h}$ and

then neutralized with a few drops of TEA. The solvent was removed under reduced pressure, and the product was purified via column chromatography (2:1 hexanes:ethyl acetate, 3% TEA) yielding 5.03 g of clear oil (85% yield). 500 MHz ^1H NMR spectroscopy (δ , CDCl_3 as solvent): 6.08 ppm (m, 1H, $\text{CH}_2=\text{C}(\text{CH}_3)$), 5.54 ppm (m, 1H, $\text{CH}_2=\text{C}(\text{CH}_3)$), 4.81 ppm (m, 1H, OCHO), 4.28 ppm (m, 4H, COOCH_2), 3.74 ppm (m, 4H, CH_2OCH), 1.91 ppm (m, 9H, $\text{C}(\text{CH}_3)_2\text{Br}$, $\text{CH}_2=\text{C}(\text{CH}_3)$), and 1.29 ppm (d, 3H, $\text{OCH}(\text{CH}_3)\text{O}$).

Synthesis of 3-Azido-2-hydroxypropyl Methacrylate.²⁹ In a 250 mL round-bottom flask, sodium azide (10.00 g, 0.15 mol) and sodium bicarbonate (7.50 g, 0.089 mol) were dissolved in 125 mL of water and 25 mL of THF. The mixture was then purged with nitrogen before the addition of glycidyl methacrylate (10.00 mL, 0.070 mol). The mixture was allowed to stir in the dark for 2 days. It was then extracted by DCM (50 mL, 5 times) and dried using MgSO_4 before removing the solvent under reduced pressure to collect 9.38 g of clear oil (69% yield). 500 MHz ^1H NMR spectroscopy (δ , CDCl_3 as solvent): 6.18/6.16 ppm (m, 1H, $\text{CH}_2=\text{C}(\text{CH}_3)$), 5.66/5.64 ppm (m, 1H, $\text{CH}_2=\text{C}(\text{CH}_3)$), 5.07 ppm (m, 1H, CHOH), 4.03 ppm (m, 2H, COOCH_2), 3.49 ppm (m, 2H, CH_2N_3), 2.87 ppm (s, 1H, HOCH), and 1.96 ppm (s, 3H, $(\text{CH}_3)_2\text{C}=\text{CH}_2$).

Synthesis of 3-Azido-2-((2-bromo-2-methylpropanoyl)oxy)propyl Methacrylate (Inimer 3).²⁹ 3-Azido-2-hydroxypropyl methacrylate (12.60 g, 0.068 mol) and 9.48 mL of TEA (0.068 mol) were dissolved in 75 mL of DCM before being cooled to 0 °C in an ice–water bath. 2-Bromoisobutyl bromide (8.41 mL, 0.068 mol) was dissolved in 25 mL of DCM and then slowly added to the reaction mixture over 30 min. The reaction was allowed to stir for 24 h before filtering off the solid. The reaction mixture was washed once with 1 M HCl and 1 M NaOH and then with water 5 times. A black liquid was obtained and purified using silica column chromatography (10:1 hexanes:ethyl acetate), obtaining 13.87 g of yellow oil (61% yield). 500 MHz ^1H NMR spectroscopy (δ , CDCl_3 as solvent): 6.18/6.14 (m, 1H, $\text{CH}_2=\text{C}(\text{CH}_3)$), 5.66/5.62 (m, 1H, $\text{CH}_2=\text{C}(\text{CH}_3)$), 5.27 ppm (m, 1H, HOCO), 4.38 ppm (m, 2H, COOCH_2), 3.56 ppm (m, 2H, CH_2N_3), 1.96 ppm (s, 3H, $(\text{CH}_3)_2\text{C}=\text{CH}_2$), and 1.95 ppm (m, 6H, $\text{C}(\text{CH}_3)_2\text{Br}$).

Synthesis of 2-((2-Hydroxyethyl)disulfanyl)ethyl 2-Bromo-2-methylpropanoate.²³ A 500 mL round-bottom flask equipped with a magnetic stir bar was loaded with 200 mL of DCM before being cooled to 0 °C in an ice–water bath. Bis(2-hydroxyethyl) disulfide (10.00 g, 0.065 mol) and triethylamine (TEA, 22.60 mL, 0.16 mol) were then added to the flask and stirred for 10 min before 2-bromoisobutyl bromide (7.20 mL, 0.060 mol) was slowly added to the reaction mixture using a syringe pump (10 mL syringe with 15.6 mm diameter, 1.1 mL/h, 8 h). Solid precipitant formed during the syringe pump addition, and a light pink reaction mixture was left stirring for overnight before being filtered. The obtained filtrate was sequentially washed with 200 mL of 1 M HCl, 300 mL of saturated sodium bicarbonate, and 300 mL of saturated ammonium chloride before being dried with magnesium sulfate. The product (yield of 15.26 g) was directly used in reaction with methacryloyl chloride for the synthesis of inimer 4. Any contaminant of dibromo compound was later removed from the final product using silica column chromatography. 500 MHz ^1H NMR spectroscopy (δ , CDCl_3 as solvent): 4.43 ppm (t, 2H, COOCH_2), 3.87 ppm (t, 2H, HOCH_2), 2.95 ppm (t, 2H, $\text{SCH}_2\text{CH}_2\text{OCO}$), 2.87 ppm (t, 2H, $\text{SCH}_2\text{CH}_2\text{OH}$) and 1.92 ppm (s, 6H, $\text{C}(\text{CH}_3)_2\text{Br}$).

Synthesis of 2-((2-((3-Methyl-2-oxobut-3-en-1yl)xy)ethyl)disulfanyl)ethyl 2-Bromo-2-methyl propanoate (Inimer 4).³⁰ 2-((2-Hydroxyethyl)disulfanyl)ethyl 2-bromo-2-methylpropanoate (10.00 g, 0.033 mol) and TEA (14.00 mL, 0.10 mol) were dissolved in 100 mL of DCM in a 250 mL round-bottom flask equipped with magnetic stir bar. The mixture was then cooled to 0 °C in an ice–water bath, and methacryloyl chloride (9.70 mL, 0.10 mol) was slowly added over 25 min via an addition funnel. The mixture turned into a vibrant red-orange color upon the addition and was allowed to stir overnight at room temperature with solid precipitant formed during the reaction. The mixture was then washed with 250 mL of 1 M HCl (turning bright red) and 300 mL of 1 M NaOH (turning pale yellow), before being dried with MgSO_4 . Solvent was then removed under reduced pressure, and the product was purified on a silica column (9:1 hexanes:ethyl acetate),

collecting 6.85 g of light yellow oil (56% yield). 500 MHz ^1H NMR spectroscopy (δ , CDCl_3 as solvent): 6.08 ppm (m, 1H, $\text{CH}_2=\text{C}(\text{CH}_3)$), 5.53 ppm (m, 1H, $\text{CH}_2=\text{C}(\text{CH}_3)$), 4.35 ppm (m, 4H, CH_2O), 2.90 ppm (m, 4H, CH_2S), 1.95 ppm (s, 3H, $\text{CH}_2=\text{C}(\text{CH}_3)$), and 1.90 ppm (s, 6H, $\text{C}(\text{CH}_3)_2\text{Br}$).

Synthesis of 3-Azido-2-((2-((2-bromo-2-methylpropanoyl)oxy)ethoxy)ethoxy)propyl Methacrylate (Inimer 5). 3-Azido-2-hydroxypropyl methacrylate (2.73 g, 0.015 mol) and 2-((vinylloxy)ethyl 2-bromo-2-methylpropanoate (3.50 g, 0.015 mol) were dissolved in 70 mL of DCM. Catalytic amount of *p*-toluenesulfonic acid (28.0 mg, 0.15 mmol) was added to start the reaction. The reaction was left to stir for 1.5 h and then neutralized with a few drops of TEA. The product was purified via column chromatography (4:1 hexanes:ethyl acetate with 3 vol % TEA), collecting 2.92 g of clear oil (47% yield). 500 MHz ^1H NMR spectroscopy (δ , CDCl_3 as solvent): 6.11/6.07 ppm (m, 1H, $\text{CH}_2=\text{C}(\text{CH}_3)$), 5.59/5.56 ppm (m, 1H, $\text{CH}_2=\text{C}(\text{CH}_3)$), 4.91 ppm (m, 1H, OCHO), 4.15 ppm (m, 5H, COOCH_2 , CH_2CHO), 3.59 ppm (m, 4H, CH_2N_3 , OCH_2), 1.92 ppm (s, 3H, $(\text{CH}_3)_2\text{C}=\text{CH}_2$), 1.90 ppm (m, 6H, $\text{C}(\text{CH}_3)_2\text{Br}$), and 1.32 ppm (m, 3H, $\text{OCH}(\text{CH}_3)\text{O}$).

Microemulsion Polymerization of Inimers. All experimental procedures for synthesis of hyperbranched polymers in microemulsion had similar conditions. A typical procedure for the polymerization of inimer 1 with $[\text{inimer } 1]_0/[\text{CuBr}_2]_0/[\text{dNbpy}]_0/[\text{NaAs}]_0 = 70/1/2/0.5$ is briefly described. In a disposable test tube, dNbpy (10.6 mg, 0.026 mmol) and CuBr_2 (2.9 mg, 0.013 mmol) were mixed in 0.5 mL of DCM at 40 °C for half an hour before addition of inimer 1 (0.25 g, 0.90 mmol) to the mixture. After evaporation of the DCM at 40 °C, the mixture was added dropwise to a solution of 1 g of Brij98 in 12 g of water over 30 min to form a transparent microemulsion. Meanwhile, the temperature was slowly stepped up to 65 °C and stabilized for less than 10 min before injection of 0.10 mL of NaAs solution in water to reduce the Cu(II) species and initiate the polymerization. At timed intervals, samples were withdrawn via a syringe fitted with stainless steel needle and dried in an aluminum tray. SEC samples were dissolved in THF, passed through a short alumina column to remove copper, and filtered through 0.45 μm PTFE filter. NMR spectroscopy samples were directly dissolved in CDCl_3 for analysis. The reaction was stopped after 2 h, and the product was isolated by addition of THF into microemulsion, followed by centrifugation. The isolated polymer was further purified by dissolved in THF and then precipitated out in methanol to remove the surfactant.

Degradation of Acetal-Containing Hyperbranched Polymer. A mixture of 2:1:1 of acetic acid:trifluoroacetic acid:water (0.40 mL) was added to a polymer solution in acetone (50.0 mg of polymer in 1.00 mL). Once the degradation was complete, 10 mL of saturated sodium bicarbonate was added to the polymer solution and then extracted with 10 mL of DCM three times. The mixture was dried with magnesium sulfate and reduced to yield the degraded mixture.

Solution Polymerization. A typical procedure on the polymerization of inimer 3 using normal ATRP consisted of $[\text{inimer } 3]_0/[\text{CuBr}_2]_0/[\text{dNbpy}]_0 = 70/1/2$ is briefly described. In a 10 mL Schlenk flask, inimer 3 (0.25 g, 0.75 mmol) and dNbpy (8.7 mg, 0.021 mmol) were dissolved in 0.60 mL of toluene. The flask was deoxygenated by five freeze–pump–thaw cycles. During the final cycle, the flask was filled with nitrogen before CuBr (1.5 mg, 0.011 mmol) was quickly added to the frozen mixture. The flask was sealed with a glass stopper and then evacuated and backfilled with nitrogen five times before it was immersed in an oil bath at 65 °C. The reaction conversion was monitored by ^1H NMR spectroscopy, and the reaction was stopped after >98% conversion. The solution was filtered through a column filled with neutral alumina, and the final polymer was obtained after precipitation into methanol.

Bulk Polymerization. A typical procedure on the bulk polymerization of inimer 1 using AGET ATRP consisted of $[\text{inimer } 1]_0/[\text{CuBr}_2]_0/[\text{dNbpy}]_0/[\text{tin(II) 2-ethylhexanoate}]_0 = 70/1/2/0.5$ is briefly described. Inimer 1 (0.50 g, 1.79 mmol), dNbpy (20.9 mg, 0.051 mmol), and CuBr_2 (5.7 mg, 0.026 mmol) were loaded in a 10 mL Schlenk flask. The flask was deoxygenated by five freeze–pump–thaw cycles and immersed in an oil bath at 65 °C before the addition of tin(II) 2-ethylhexanoate (4.1 μL , 0.013 mmol). The reaction conversion was

Scheme 2. Molecular Structures of Inimers

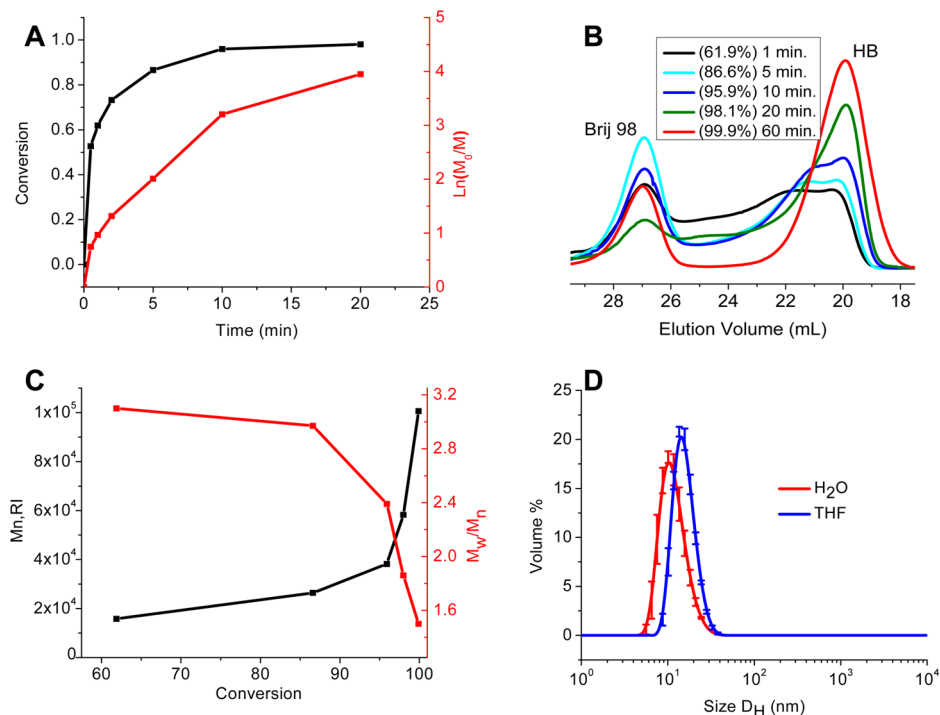
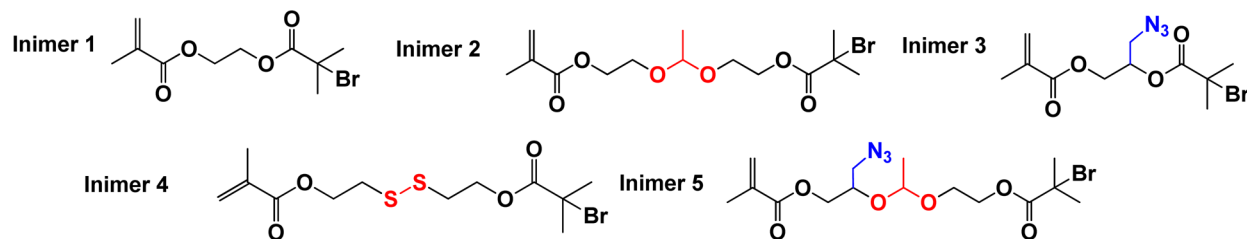


Figure 1. (A) Dependence of inimer **1** conversion and $\ln([M_0]/[M])$ on reaction time determined by ^1H NMR spectroscopy. (B) SEC traces of minimally purified HB1 polymers at different conversions. (C) Relative molecular weight and M_w/M_n versus conversion of methacrylate groups. (D) DLS curves of HB1 in latex before purification and in THF after purification.

monitored by ^1H NMR spectroscopy, and the reaction reached macroscopic gelation at ~65% conversion.

RESULTS AND DISCUSSION

This work advances our present microemulsion polymerization method to yield a library of hyperbranched polymers with various chemical compositions, narrow molecular weight distributions, tunable molecular weights, and high DBs. Five methacrylate-based inimers that contain different spacer groups (Scheme 2) were applied in the atom transfer radical polymerization (ATRP) in microemulsion.³¹ Brij98, a nonionic surfactant, was used as the emulsifier (1 g of Brij98 per 0.25 g of inimer), which gave the best microemulsion stability for all inimers in the ATRP condition.³² Activators generated by electron transfer (AGET)^{30,31} were applied as the initiation technique because it starts with air-stable Cu(II) species,³³ which is critical for a heterogeneous ATRP reaction. Hydrophobic ligands, dNbpy³⁴ and BPMODA,³⁵ were used to complex copper salts and minimize their partitioning into the aqueous phase.

AGET ATRP of inimer **1** in microemulsion showed fast polymerization with the conversion of methacrylate double bonds reaching 98% within 20 min (Figure 1A). In contrast, most literature reports on the polymerization of inimers in dilute conditions often required hours or even days to achieve complete

conversions and polymers with high molecular weights.^{36–39} The fast inimer polymerization in the microemulsion droplets was mainly due to the concentration effect without dilution since parallel AGET ATRP of inimer **1** in bulk exhibited similar polymerization rate at initial stage before quickly turning into a macroscopic gel in a minute. At the same time, leakage of copper catalyst into aqueous phase should also be counted as a factor to alter the ratio of Cu(I) and Cu(II) species in the polymerizing particles. Although hydrophobic ligands, such as dNbpy and BPMODA, were used in the microemulsion polymerization, previous studies of ATRP in aqueous dispersed media demonstrated that some amount of copper catalysts did leak into the aqueous phase.³³ A higher partition of Cu(II) in water than Cu(I) complexes can decrease the effective concentration of Cu(II) deactivator in the discrete particles more significantly, which increases the polymerization rate and lowers the DB value, as will be discussed later.

Figure 1B shows the molecular weight evolution of hyperbranched polymers after removing most of the surfactant but with minimal polymer fractionation. It was found that polymers with broad molecular weight distribution ($M_w/M_n \sim 3.1$) were initially formed at low conversion (~62% at 1 min). As the reaction progressed, these hyperbranched polymers showed a

Table 1. Hyperbranched Polymers Produced by AGET ATRP of Inimers in Microemulsion^a

polymer	ligand	$M_{n,MALLS}^b$ ($\times 10^3$)	$M_{n,RI}^c$ ($\times 10^3$)	M_w/M_n^c (RI)	$D_h(H_2O)^d$ (nm)	$D_h(THF)^d$ (nm)	CV^d	DB^e
HB1	dNbpy	301	101	1.4	12.61	13.34	0.13	0.31 \pm 0.03
HB2	dNbpy	595	102	1.1	12.11	14.61	0.09	0.41 \pm 0.05
HB3	dNbpy	219	55.4	1.3	14.27	15.44	0.13	0.41 \pm 0.05
HB4	dNbpy	243	63.9	1.3	10.95	13.09	0.12	0.37 \pm 0.07
HB5	dNbpy	194	62.4	1.2	12.04	13.18	0.11	0.41 \pm 0.02
HB1*	BPMODA	1216	140	1.3	14.24	21.71	0.12	0.28 \pm 0.02
HB2*	BPMODA	1301	109	1.5	16.04	20.02	0.14	0.26 \pm 0.02
HB3*	BPMODA	1056	104	1.6	16.28	33.65	0.15	0.33 \pm 0.01
HB4*	BPMODA	1102	127	1.4	20.13	32.40	0.11	0.35 \pm 0.01
HB5*	BPMODA	1115	118	1.6	17.54	31.52	0.16	0.35 \pm 0.02

^aExperimental conditions: [inimer]₀: [CuBr₂]₀: [dNbpy]₀: [NaAs]₀ = 70:1:2:0.5 or [inimer]₀: [CuBr₂]₀: [BPMODA]₀: [NaAs]₀ = 70:1:1:0.5, weight ratio of inimer to Brij98 = 1:4, 1 g of Brij98 in 12 g of water, 65 °C, 2 h. ^bNumber-average molecular weight measured by THF SEC with MALLS detector. ^cApparent number-average molecular weight and molecular weight distribution measured by THF SEC with RI detector, calibrated with linear PMMA standards. ^dVolume average hydrodynamic diameter (D_h) and coefficient of variation (CV) determined by DLS using PMMA refractive index. ^eDegree of branching (DB) determined by integration of peaks in inverse gated decoupled ¹³C NMR spectra.

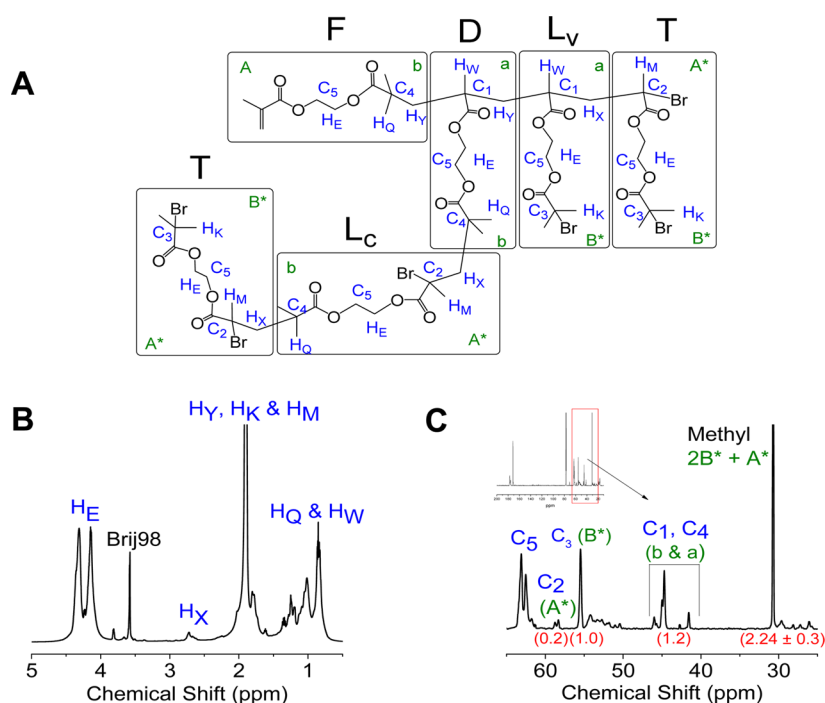
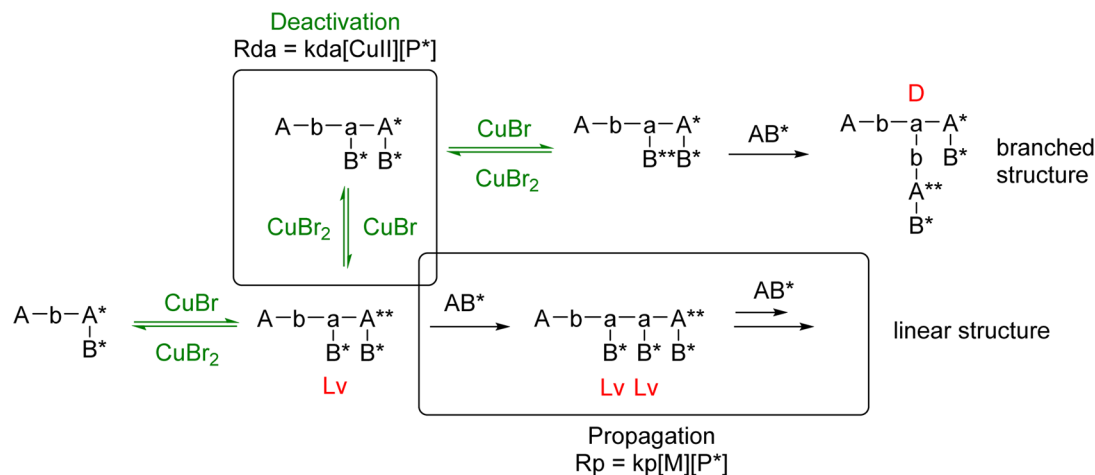


Figure 2. (A) A representative structure of HB1 containing five structural units: focal (F), dendritic (D), terminal (T), and linear (linear vinyl L_v , linear condensation L_c) units; five subunits: unreacted double bond (A), initiating site from reacted double bond (A*), unreacted initiating site (B*), reacted double bond (a), and reacted initiating site (b). (B) ¹H NMR spectrum of HB1 with peak assignment. (C) Inverse gated decoupled ¹³C NMR spectrum of HB1 with peak assignments, determined by 2-D HSQC and HMBC spectroscopy.

sharp increase of molecular weight and a decreased polydispersity (Figure 1C). The sharp increase of molecular weight at high conversion was in agreement with the step-growth mechanism. However, the decreased polydispersity was not common in a hyperbranched polymer synthesis. A reasonable hypothesis is that there were multiple polymer molecules present in the polymerizing droplet at low conversion. These polymer molecules containing both polymerizable group and initiating groups would react with each other (polymer–polymer reaction) with the progress of polymerization and finally formed a single hyperbranched macromolecule at complete conversion. The dimension and uniformity of the discrete droplet directly regulate the molecular weight and polydispersity of hyperbranched polymers. Because of the relatively uniform distribution of the micelles in microemulsion, the final hyperbranched

polymer HB1 after complete conversion exhibited a high molecular weight ($M_{n,MALLS}$ = 301 kg/mol and $M_{n,RI}$ = 101 kg/mol, Table 1) and low polydispersity (M_w/M_n = 1.4). This hypothesis was further supported by DLS measurements of the polymer in latex before purification and in THF after purification (Figure 1D). The polymers after dissolved in THF showed increased hydrodynamic size as compared to the D_h of latexes in water, confirming that there was one polymer molecule per latex nanoparticle. Otherwise, the purified hyperbranched polymer after dissolved in the good solvent would fall into smaller fragments with decreased hydrodynamic size.

Branching density, i.e., DB, one of the most important structural parameters in hyperbranched polymers, is essential for accurate and complete characterization. However, the complex structure of hyperbranched polymers with the presence of many

Scheme 3. Dynamic Exchange Process during ATRP of Inimer^a

^aA** and B** represent propagating radicals. All other designated letters are the same as those in the Figure 2 caption.

structural units in one macromolecule poses challenges to the characterization.^{40,41} A recent study in our group²³ used ¹H NMR spectroscopy with the aid of a set of five equations to quantify the fraction of subunits in the hyperbranched polymers and calculated the relative reactivity ratio of $r = k_{A^*}/k_{B^*}$.⁴² However, the integration accuracy in the ¹H NMR spectrum has not been verified due to the significant overlap of broad signals. Inverse gated ¹³C NMR spectroscopy, coupled with HSQC and HMBC spectroscopy, has previously been applied to determine the DB of complex polymer structures, demonstrating advantages of well-resolved intricate NMR signals.^{19,43–45} This technique was applied in our current study to quantify the DB values of all methacrylate-based hyperbranched polymers produced from the SCVP of inimers in microemulsion.

After careful peak assignment in the ¹H and ¹³C NMR spectra with the aid of small molecules and linear PMMA polymers (see Supporting Information, Figures S6 and S7 for details), integration of the peaks in Figure 2C was applied to calculate the DB of HB1. Since the conversion of methacrylate groups in inimer 1 was >98% after polymerization, a complete conversion of conv = 1 was applied to simplify the calculation.⁴⁶ Without considering intermolecular cyclization or radical termination, the number of A* subunits equals the number of b ($N_{A^*} = N_b$) and the number of B* subunit equals the sum of a and A ($N_{B^*} = N_a + N_A$), which agrees well with the peak integration result in Figure 2C (peak areas of C2 and C3 equaled those of C1 and C4). Using this relationship, the number fraction of B* subunit was determined as $f_{B^*} = N_{B^*}/(N_{B^*} + N_b) = 0.81$, which was then used to calculate the reactivity ratio ($r = k_{A^*}/k_{B^*} = (\text{conv}_A + f_{B^*} - 1)/(-\ln f_{B^*} + f_{B^*} - 1) = 39$) and a DB = 0.31 (see Supporting Information, section 2).^{46,47} An alternative method of integrating the methyl carbon peak at 30 ppm (two -CH₃ groups from B* subunit and one -CH₃ from A* subunit) and the quaternary carbon peak at 55 ppm (B* subunit) could also determine the DB value of HB1 as DB = 0.31, confirming the integration accuracy. It is worth mentioning that similar method was applied to calculate the DB of hyperbranched polymer HB1* that was synthesized by using BPMODA as ligand in microemulsion. The result of DB_{HB1*} = 0.28 was very close to the previously reported DB = 0.27 based on the analysis of ¹H NMR spectrum.²³

It was also noticed that the experimental DB value of HB1 (DB_{HB1} = 0.31) was lower than the theoretical value (DB_{theor} = 0.48–0.43), which was calculated using the literature reactivity

ratio of $r = k_{A^*}/k_{B^*} = 5–10$ in inimer 1.⁴⁸ Since the ratio of $r = k_{A^*}/k_{B^*}$ is an apparent value, determined not only by the activation rates of these two groups (A* and B*) in ATRP but also by the propagation and deactivation rates of the corresponding radicals,⁴⁹ the discrepancy between the theoretical and experimental DB values could be a symptom of the leakage of catalyst into the aqueous phase.³⁴ Despite the use of a hydrophobic ligand dNbpy, copper complexes, particularly the Cu(II)/(dNbpy)₂ could still exit the discrete polymerizing particles into water,⁵⁰ resulting in a decreased deactivation.

Scheme 3 illustrates the competition between the propagation and deactivation reactions in the ATRP of inimer, which is critical to mediate the branching process. A propagating radical formed from the activation of alkyl halide could either react with a new inimer to form a linear unit (such as Lv) or be deactivated by reacting with Cu(II) deactivator. Without adequate deactivator, the increased rate ratio of propagation over deactivation would produce more linear units from one radical in an activation/deactivation cycle and lower the DB of polymers. In contrast, a fast deactivation reaction could quickly stop the propagation of linear units and raise the chance of activating a different alkyl halide in another activation/deactivation cycle, which is the essential step to form a branched unit (D in Scheme 3). To prove this idea, two solution polymerizations of inimer 1 in toluene with initial molar ratios of CuBr₂/(dNbpy)₂ to inimer as 1:70 and 1:140 were set up, in which all copper catalysts were well dissolved and their concentrations in solution were determined by the feed amounts. After stopping the polymerizations at high conversion, the hyperbranched polymers using more added CuBr₂/(dNbpy)₂ had a high DB = 0.46 ± 0.02 (within the range of DB_{theor} = 0.48–0.43). As comparison, the hyperbranched polymer using less CuBr₂/(dNbpy)₂ showed a low DB = 0.26 ± 0.07 (Figures S9 and S10 in the Supporting Information). This result supports the claim that a fast deactivation reaction is critical in order to produce hyperbranched polymers with high DB. By applying this principle to ATRP in microemulsion, a strategy of tuning DB is to control the effective concentration of deactivator in the dispersed oil phase.

Effect of Catalyst Solubility on Polymer DB. In the current study, all five inimers contained a methacrylate polymerizable group and a tertiary alkyl bromide initiating group. Without considering other factors, these inimers were expected to polymerize in similar manner and produce

Table 2. Effect of Catalyst Amounts on the Structures of HB3^a

inimer (g)	[inimer] ₀ : [CuBr ₂] ₀	<i>M</i> _{n,MALLS} ^b (×10 ³)	<i>M</i> _{n,RI} ^c (×10 ³)	<i>M</i> _w / <i>M</i> _n ^c (RI)	<i>D</i> _h (H ₂ O) ^d (nm)	<i>D</i> _h (THF) ^d (nm)	CV ^d	DB ^e
0.25	70:1	219	55.4	1.3	14.27	15.44	0.13	0.41 ± 0.05
0.25	100:1	255	61.1	1.3	11.46	12.28	0.14	0.36 ± 0.04
0.25	140:1	246	59.2	1.7	11.75	13.36	0.15	0.20 ± 0.08

^aExperimental conditions: [CuBr₂]₀: [dNbpy]₀: [NaAs]₀ = 1:2:0.5, 1 g of Brij98 in 12 g of water, 65 °C, 2 h. ^bNumber-average molecular weight measured by THF SEC with MALLS detector. ^cApparent number-average molecular weight and molecular weight distribution measured by THF SEC with RI detector, calibrated with linear PMMA standards. ^dVolume average hydrodynamic diameter (*D*_h) and coefficient of variation (CV) determined by DLS using PMMA refractive index. ^eDegree of branching (DB) determined by integration of peaks in inverse gated decoupled ¹³C NMR spectra.

Table 3. Effect of Inimer Amounts on HB1 Structures^a

inimer (g)	[inimer] ₀ : [CuBr ₂] ₀	<i>M</i> _{n,MALLS} ^b (×10 ³)	<i>M</i> _{n,RI} ^c (×10 ³)	<i>M</i> _w / <i>M</i> _n ^c (RI)	<i>D</i> _h (H ₂ O) ^d (nm)	<i>D</i> _h (THF) ^d (nm)	CV ^d	DB ^e
0.15	70:1	268	95.1	1.2	11.64	13.70	0.15	0.34 ± 0.06
0.20	70:1	294	98.7	1.2	12.38	13.68	0.14	0.31 ± 0.01
0.25	70:1	301	101	1.4	12.61	13.34	0.13	0.31 ± 0.03
0.30	70:1	370	121	1.4	13.45	17.78	0.14	0.31 ± 0.01

^aExperimental conditions: [inimer 1]₀: [CuBr₂]₀: [dNbpy]₀: [NaAs]₀ = 70:1:2:0.5, 1 g of Brij98 in 12 g of water, 65 °C, 2 h. ^bNumber-average molecular weight measured by THF SEC with MALLS detector. ^cApparent number-average molecular weight and molecular weight distribution measured by THF SEC with RI detector, calibrated with linear PMMA standards. ^dVolume-average hydrodynamic diameter (*D*_h) and coefficient of variation (CV) determined by DLS using PMMA refractive index. ^eDegree of branching (DB) determined by integration of peaks in inverse gated decoupled ¹³C NMR spectra.

hyperbranched polymers with similar DBs. However, the different linker groups in these inimers changed their structures and the solubility of copper catalyst in them and consequently altered the deactivation rate in each microemulsion polymerization. For instance, CuBr₂/(dNbpy)₂ exhibited dramatic solubility difference in inimers 1 and 3 (i.e., 1.33 vs 2.32 mg/g at 25 °C), which resulted in the DB difference in the two produced hyperbranched polymers, DB_{HB1} = 0.31 vs DB_{HB3} = 0.41 (Table 1). At the same time, the polymerization rates in both microemulsion polymerizations were similar, and both reached >98% conversion within 20 min. Thus, the solubility difference of copper catalysts in these two inimers merely changed the overall concentrations of catalysts but did not significantly vary the ratio of Cu(I)/Cu(II) in these two systems. By changing the inimer species, we were able to tune the DB value of hyperbranched polymers without affecting polymerization rate. When inimer 3 was used, the produced hyperbranched polymer showed a DB_{HB3} = 0.41, approaching the theoretical value of methacrylate-based inimer (DB_{theor} = 0.48–0.43).

In ATRP, N-containing ligands not only play a significant role on tuning the reactivity of catalysts but also alter the solubility of the copper complexes in the media. In our study, two hydrophobic ligands, tridentate BPMODA and bidentate dNbpy, were used and showed different copper complex solubility. For instance, the solubility of CuBr₂/(dNbpy)₂ complex in inimer 3 was 2.32 mg/g at 25 °C, 3 times higher than that of CuBr₂/BPMODA complex in inimer 3 (0.78 mg/g) under same temperature. This difference significantly affected the DBs of hyperbranched polymers with results of DB_{HB3} = 0.41 vs DB_{HB3*} = 0.33 in Table 1. Across all of the inimer species within our study, the DBs of hyperbranched polymers when using BPMODA as the ligand were always lower than those using dNbpy as the ligand (Table 1). Since the copper complexes with these two ligands have similar reactivities (similar activation rate constants and ATRP equilibrium constants),⁵¹ the DB difference of the polymers by changing ligands was mainly due to the lower solubility of copper complexes with BPMODA than with dNbpy.

Effect of Catalyst Amount on Polymer DB. Since dNbpy ligand provides high solubility of copper catalyst in inimer 3, an initial feed ratio of [CuBr₂]/(dNbpy)₂ to [inimer 3]₀ = 1:70 produced hyperbranched polymer with DB_{HB3} = 0.41, close to the theoretical value. Decrease of the feed ratios of [CuBr₂]/(dNbpy)₂ to [inimer 3]₀ to 1:100 and 1:140 in 0.25 g of inimer 3 lowered down the DB of hyperbranched polymer to respective 0.36 and 0.20, without significantly changing the size and molecular weights of the polymers (Table 2). As expected, less catalyst in the confined loci slowed the exchange reactions between active radicals and dormant alkyl bromides, leading to a low fraction of dendritic units, as shown in Scheme 3.

Hyperbranched Polymers with Tunable Compositions.

The presence of a linker between the polymerizable group and initiating group in the inimer provides opportunity to introduce functional groups into the inimers and the hyperbranched polymers. In this study, five inimers with different linker groups, including acetal, disulfide, and azide groups, were applied in the microemulsion ATRP and produced hyperbranched polymers containing reactive groups and degradable groups in the backbone. All polymerizations in microemulsion were fast and reached high conversion (>98%) within 0.5 h. The produced hyperbranched polymers showed monomodal peaks in DLS with larger hydrodynamic sizes in THF after purification than the latexes in water, indicating one hyperbranched polymer per polymerized micelle after reaction. Slight variation of hydrodynamic size and polydispersity of the polymers was probably due to the emulsification features of different inimers and catalysts, in which the use of BPMODA as ligand often required longer microemulsification process and produced polymers with higher molecular weight and less uniform structure. In Table 1, the five hyperbranched polymers HB1–HB5 using dNbpy as ligand showed hydrodynamic sizes of *D*_h = 15–21 nm in THF and absolute molecular weights of *M*_{n,MALLS} < 600 kg/mol. In contrast, hyperbranched polymers HB1*–HB5* using BPMODA as ligand had *D*_h between 30 and 40 nm in THF and absolute molecular weights over 1000 kg/mol. Between these two ligands, dNbpy is capable of producing hyperbranched polymers with lower molecular weights and more uniform structures than

BPMODA. Overall, the microemulsion ATRP method that polymerizes inimer in confined micellar space has demonstrated its robustness to synthesize a variety of hyperbranched polymers with different compositions, tunable DBs, and relatively low polydispersity.

Tuning Molecular Weights of Hyperbranched Polymers. To investigate the effect of solid contents in microemulsion on the molecular weight of hyperbranched polymers, three ATRPs of inimer **1** using dNbpy as ligand but varied amounts of inimer were carried out (Table 3). Increasing the loading amounts of inimer from 0.15 to 0.3 g increased the size of latexes after polymerization from 11.64 to 13.45 nm, a 15% size increase corresponding to 150% increase in volume. After purification to remove the surfactant, the hyperbranched polymers dissolved in THF showed an increase of absolute molecular weights from 268 to 370 kg/mol, representing a 1.4 times increase. Since the number of empty micelles in a microemulsion polymerization significantly outweighs the number of polymerized micelles (ca. 99%:1%),^{52,53} doubling the loading amount of inimers increased not only the size of each polymerized micelle but also the fraction of latexes versus empty micelles, resulting in a disproportional increase of molecular weight with solid contents.

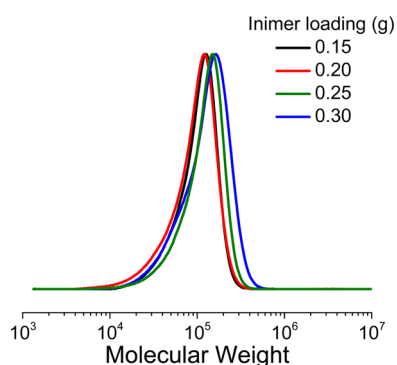


Figure 3. SEC of a series of hyperbranched polymers HB1 synthesized with different feed amounts of inimer **1**.

Degradation of Hyperbranched Polymers. Hyperbranched polymers with well-defined structures and degradability under mild conditions can potentially be used in delivery of therapeutic compounds.^{5,33,54} To demonstrate the degrad-

ability of our hyperbranched polymers, an acetal-containing HB2 polymer was applied to an acidic condition to investigate the degradation process.²⁰ Figure 4 shows the progress of degradation of HB2 polymer in acidic conditions. A series of ¹H NMR spectra by tracking the proton in acetal groups indicate that the degradation was complete within 800 min with 100% conversion of acetal groups (Figure 4A,B). Preliminary characterization of each fraction in the SEC curve using LC-MS indicates the final degraded product was mainly composed of small molecules, such as 2-hydroxyethyl 2-bromoisobutyrate, 2-hydroxyethyl methacrylate, and some oligomeric species (Figure 4C). Thus, the current method of one-pot polymerization of inimer in microemulsion demonstrates versatility to produce hyperbranched polymers that show features of degradability, high molecular weights, and narrow size distribution in one entity.

CONCLUSIONS

This paper presents a systematic study of our recent development that used microemulsion to regulate the molecular structure of hyperbranched polymers in the one-pot ATRP of inimers. The dispersed micellar droplets, behaving as discrete templates, segregate the polymerization and the polymer–polymer reactions within individual loci. At high conversion of inimers, there was only one hyperbranched polymer in each confined polymerizing nanoparticle, which showed a high molecular weight and uniform structure. Five methacrylate-based inimers containing different functional linkers were successfully applied in the microemulsion ATRP to produce series of hyperbranched polymers with tunable chemical compositions, molecular weights, and DBs. Within our investigation, all polymerizations showed fast rate with >98% conversions achieved within half an hour. Structural characterization of these hyperbranched polymers using inverse gated ¹³C NMR spectroscopy determined the DB of polymers in the range of 0.20–0.41, and the value was critically influenced by several parameters, including the inimer species, the ATRP ligand structure, and the feed ratio of copper catalyst to inimer. Hyperbranched polymers with high DB values could be produced via (1) increasing the solubility of Cu(II) deactivator in the dispersed droplets using proper inimers and ligands or (2) using high feed ratio of copper catalyst to inimer. Within the study, the polymerization of inimer **3** using dNbpy as ligand and

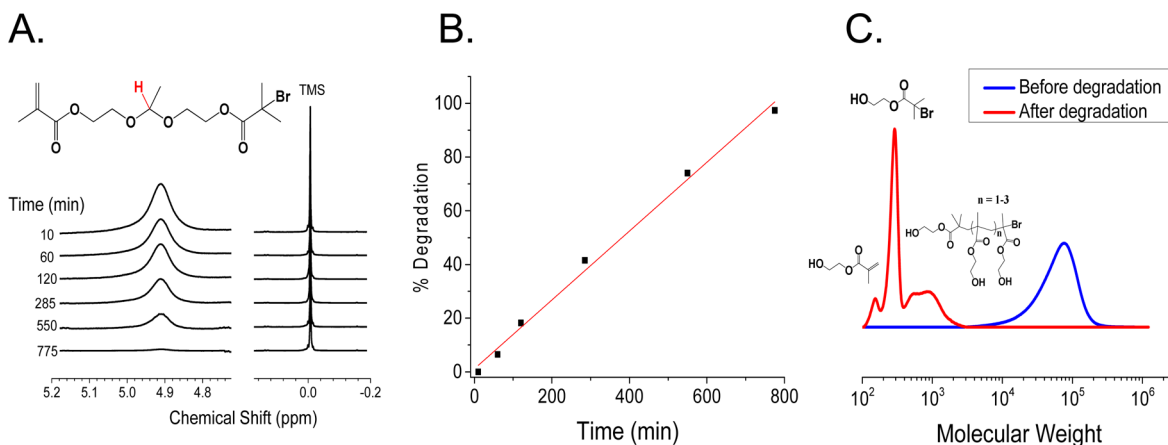


Figure 4. (A) ¹H NMR spectra of the degraded product of HB2 as a function of time with respect to standard TMS peak. (B) Percentage of degraded acetal bond in the polymer over time. (C) SEC trace of hyperbranched polymer before and after degradation.

$[\text{CuBr}_2]_0: [\text{inimer } 3]_0 = 1:70$ produced a hyperbranched polymer with $\text{DB} = 0.41$, approaching the theoretical value of $\text{DB}_{\text{theor}} = 0.48\text{--}0.43$. When inimer **2** containing an acetal linker group was used, the produced hyperbranched polymer exhibited complete degradation in acidic environment into small molecular fragments. These results demonstrated the robustness of this new synthetic method on regulating the synthesis of hyperbranched polymers in one-pot. As compared to reported methods that used slow addition/core dilution or special monomers with unequal reactivities, our current method represents a facile strategy to produce hyperbranched polymers with high molecular weights, low polydispersity, and a range of functionalities.

■ ASSOCIATED CONTENT

Supporting Information

Figures S1–S11. This material is available free of charge via the Internet at <http://pubs.acs.org>.

■ AUTHOR INFORMATION

Corresponding Author

*E-mail: hgao@nd.edu (H.G.).

Notes

The authors declare no competing financial interest.

■ ACKNOWLEDGMENTS

The authors thank the ARO YIP Award (W911NF-14-1-0227) and ACS Petroleum Research Fund (PRF #54298-DN17) for financial support. H. Gao thanks the startup support from the University of Notre Dame and the Center for Sustainable Energy at Notre Dame.

■ REFERENCES

- (1) Bosman, A. W.; Janssen, H. M.; Meijer, E. W. *Chem. Rev.* **1999**, *99*, 1665.
- (2) Grayson, S. M.; Fréchet, J. M. J. *Chem. Rev.* **2001**, *101*, 3819.
- (3) Gao, C.; Yan, D. *Prog. Polym. Sci.* **2004**, *29*, 183.
- (4) Voit, B. I.; Lederer, A. *Chem. Rev.* **2009**, *109*, S924.
- (5) Wilms, D.; Stiriba, S. E.; Frey, H. *Acc. Chem. Res.* **2010**, *43*, 129.
- (6) Tomalia, D. A.; Baker, H.; Dewald, J.; Hall, M.; Kallos, G.; Martin, S.; Roeck, J.; Ryder, J.; Smith, P. *Polym. J.* **1985**, *17*, 117.
- (7) Hawker, C. J.; Fréchet, J. M. J. *J. Am. Chem. Soc.* **1990**, *112*, 7638.
- (8) Hawker, C. J.; Lee, R.; Fréchet, J. M. J. *J. Am. Chem. Soc.* **1991**, *113*, 4583.
- (9) Segawa, Y.; Higashihara, T.; Ueda, M. *Polym. Chem.* **2013**, *4*, 1746.
- (10) Schaefgen, J. R.; Flory, P. J. *J. Am. Chem. Soc.* **1948**, *70*, 2709.
- (11) Poetzsch, R.; Komber, H.; Stahl, B. C.; Hawker, C. J.; Voit, B. I. *Macromol. Rapid Commun.* **2013**, *34*, 1772.
- (12) Fréchet, J. M. J.; Henmi, M.; Gitsov, I.; Aoshima, S.; Leduc, M. R.; Grubbs, R. B. *Science* **1995**, *269*, 1080.
- (13) Müller, A. H. E.; Yan, D.; Wulkow, M. *Macromolecules* **1997**, *30*, 7015.
- (14) Gaynor, S. G.; Edelman, S.; Matyjaszewski, K. *Macromolecules* **1996**, *29*, 1079.
- (15) Flory, P. J. *J. Am. Chem. Soc.* **1952**, *74*, 2718.
- (16) Hölter, D.; Burgath, A.; Frey, H. *Acta Polym.* **1997**, *48*, 30.
- (17) Pocovi-Martinez, S.; Kemmer-Jonas, U.; Perez-Prieto, J.; Frey, H.; Stiriba, S. E. *Macromol. Chem. Phys.* **2014**, *215*, 2311.
- (18) Sunder, A.; Hanselmann, R.; Frey, H.; Mulhaupt, R. *Macromolecules* **1999**, *32*, 4240.
- (19) Schull, C.; Rabbel, H.; Schmid, F.; Frey, H. *Macromolecules* **2013**, *46*, 5823.
- (20) Bharathi, P.; Moore, J. S. *Macromolecules* **2000**, *33*, 3212.
- (21) Ohta, Y.; Fujii, S.; Yokoyama, A.; Furuyama, T.; Uchiyama, M.; Yokozawa, T. *Angew. Chem., Int. Ed.* **2009**, *48*, 5942.
- (22) Ohta, Y.; Kamijyo, Y.; Yokoyama, A.; Yokozawa, T. *Polymers (Basel, Switz.)* **2012**, *4*, 1170.
- (23) Min, K.; Gao, H. F. *J. Am. Chem. Soc.* **2012**, *134*, 15680.
- (24) Xia, J. H.; Matyjaszewski, K. *Macromolecules* **1999**, *32*, 2434.
- (25) Gao, H.; Tsarevsky, N. V.; Matyjaszewski, K. *Macromolecules* **2005**, *38*, 5995.
- (26) Sumerlin, B. S.; Neugebauer, D.; Matyjaszewski, K. *Macromolecules* **2005**, *38*, 702.
- (27) Matyjaszewski, K.; Gaynor, S. G.; Kulfan, A.; Podwika, M. *Macromolecules* **1997**, *30*, 5192.
- (28) Rikkou-Kalourkoti, M.; Matyjaszewski, K.; Patrickios, C. S. *Macromolecules* **2012**, *45*, 1313.
- (29) Gao, C.; Zheng, X. *Soft Matter* **2009**, *5*, 4788.
- (30) Tsarevsky, N. V.; Huang, J.; Matyjaszewski, K. *J. Polym. Sci., Part A: Polym. Chem.* **2009**, *47*, 6839.
- (31) Matyjaszewski, K.; Pyun, J.; Gaynor, S. G. *Macromol. Rapid Commun.* **1998**, *19*, 665.
- (32) Min, K.; Gao, H. F.; Matyjaszewski, K. *J. Am. Chem. Soc.* **2006**, *128*, 10521.
- (33) Qiu, J.; Pintauer, T.; Gaynor, S. G.; Matyjaszewski, K.; Charleux, B.; Vairon, J. P. *Macromolecules* **2000**, *33*, 7310.
- (34) Qiu, J.; Pintauer, T.; Gaynor, S. G.; Matyjaszewski, K.; Charleux, B.; Vairon, J.-P. *Macromolecules* **2000**, *33*, 7310.
- (35) Matyjaszewski, K.; Shipp, D. A.; Qiu, J.; Gaynor, S. G. *Macromolecules* **2000**, *33*, 2296.
- (36) Dabritz, F.; Lederer, A.; Komber, H.; Voit, B. *J. Polym. Sci., Part A: Polym. Chem.* **2012**, *50*, 1979.
- (37) Muthukrishnan, S.; Mori, H.; Muller, A. H. E. *Macromolecules* **2005**, *38*, 3108.
- (38) Mori, H.; Walther, A.; Andre, X.; Lanzendorfer, M. G.; Muller, A. H. E. *Macromolecules* **2004**, *37*, 2054.
- (39) Sun, H.; Kabb, C. P.; Sumerlin, B. S. *Chem. Sci.* **2014**, *5*, 4646.
- (40) Komber, H.; Georgi, U.; Voit, B. *Macromolecules* **2009**, *42*, 8307.
- (41) Bally, F.; Ismailova, E.; Brochon, C.; Serra, C. A.; Hadzioannou, G. *Macromolecules* **2011**, *44*, 7124.
- (42) Mori, H.; Boker, A.; Krausch, G.; Muller, A. H. E. *Macromolecules* **2001**, *34*, 6871.
- (43) Nuhn, L.; Schull, C.; Frey, H.; Zentel, R. *Macromolecules* **2013**, *46*, 2892.
- (44) Lin, Y.; Dong, Z. M.; Li, Y. S. *J. Polym. Sci., Part A: Polym. Chem.* **2008**, *46*, S077.
- (45) Fischer, A. M.; Thiermann, R.; Maskos, M.; Frey, H. *Polymer* **2013**, *54*, 1993.
- (46) Yan, D. Y.; Müller, A. H. E.; Matyjaszewski, K. *Macromolecules* **1997**, *30*, 7024.
- (47) Matyjaszewski, K.; Gaynor, S. G.; Müller, A. H. E. *Macromolecules* **1997**, *30*, 7034.
- (48) Kajiwar, A.; Nanda, A. K.; Matyjaszewski, K. *Macromolecules* **2004**, *37*, 1378.
- (49) Matyjaszewski, K.; Gaynor, S. G. *Macromolecules* **1997**, *30*, 7042.
- (50) Min, K.; Matyjaszewski, K. *Macromolecules* **2005**, *38*, 8131.
- (51) Tang, W.; Kwak, Y.; Braunecker, W.; Tsarevsky, N. V.; Coote, M. L.; Matyjaszewski, K. *J. Am. Chem. Soc.* **2008**, *130*, 10702.
- (52) Hentze, H. P.; Kaler, E. W. *Curr. Opin. Colloid Interface Sci.* **2003**, *8*, 164.
- (53) Morgan, J. D.; Lusvardi, K. M.; Kaler, E. W. *Macromolecules* **1997**, *30*, 1897.
- (54) Gao, H. *Macromol. Rapid Commun.* **2012**, *33*, 722.